7 Viscous Flow of Glass Forming Liquids: Experimental Techniques for the High Viscosity Range

E.D. ZANOTTO and A.R. MIGLIORE Jr.

Department of Materials Engineering – DEMA, Federal University of São Carlos, 13565-905 São Carlos – SP, Brazil

Abstract. The viscosity is a physical parameter which controls not only the melting and fining of melts, but also the stress relaxation and the nucleation and crystallization phenomena. Here the basis of viscous flow is presented and discussed. Rheological models and some measurement methods: fiber extension, beam bending and indentation are described.

7.1 Introduction

Viscous flow governs melting, homogenization, fining, the forming operations (pressing, casting, blowing, injection molding, extrusion, etc.), and the annealing behavior of glasses and polymers. It also regulates the crystallization kinetics and consequently the thermal stability of these materials.

The viscosity reflects the intrinsic resistance to atomic or molecular translations in the liquid and, for good glass forming liquids, varies over several orders of magnitude when the temperature drops from the "liquidus" to the glass transition temperature.

In this chapter we summarize the viscous flow behavior of glass forming liquids and discuss the main experimental techniques for viscosity determinations in the upper range.

7.2 The Physics of Viscous Flow

The viscosities for a number of representative glass types are shown in Fig. 1. We stress here the great variety of glasses, ionic/covalent (SiO_2, B_2O_3), ionic (BeF_2), metallic (Pd–Au–Si), and molecular (o-Terphenyl). An important feature of the $\log(\eta)$ vs $1/T$ plots is that some of them are curved while others are straight lines (Arrhenian).

Arrhenian viscosities have only been reported for a few network (fully polymerized) inorganic glasses: silica, germania, phosphorus pentoxide, albite

Table 1. Some properties of Arrhenian network liquids [1, 2].

Glass	H_n [kJ/mol]	T_m [K]	$\log \eta(T_m)$, [Pa s]
SiO_2	520–710	1996	5.1–6.7
GeO_2	290–340	1387	3.0–5.0
P_2O_5	200	853	5.7
$NaAlSi_3O_8$	400	1380	6.9
BeF_2	240	685	5.7

Table 2. Properties on non-Arrhenian liquids.

Glass	T [K]	H_n (T_g), [kJ/mol]	H_n (T_m) [kJ/mol]
B_2O_3	546	395	85
Pd–Au–Si	620	1100	710
o-terphenyl	242	490	65

($NaAlSi_3O_8$) and beryllium fluoride, although there may be some slight curvature for germania and BeF_2. In all these glasses the higher-charged cations are tetrahedrally co-ordinated by the anions, and the anions are two-fold co-ordinated by the cations. The tetrahedra are thus linked at the vertices to form a three-dimensional continuous network. In albite the alkalis reside in holes near the aluminum ions to conserve the local charge. The constant activation enthalpies (given by the slopes of the straight lines) indicate that the structure of the (unknown) flow units of these glasses does not change appreciable with temperature. Table 1 shows the activation enthalphies (H_n) for viscous flow and the viscosities at the melting points (T_m) for these glasses [1, 2]. It should be emphasized, however, that for other network liquids such as B_2O_3, anorthite ($CaO{\cdot}Al_2O_3{\cdot}2SiO_2$) and $ZnCl_2$ the viscosity is not Arrhenian. As far as we know, Arrhenian viscosities have never been reported for polymers and metallic glasses.

For these liquids the viscosities at the melting points (of the equilibrium crystal phases) are much greater than for most liquids ($\log \eta(H_2O) = -3$; $\log \eta$ (honey) $= +1$). This is one of the reasons why the materials of Table 1 are so resistant to crystallization and thus are good glass formers.

For all other oxide, fluoride, chalcogenide, metallic, polymer and molecular glasses, for which viscosity data is available in wide temperature ranges, $\log(\eta)$ vs $1/T$ plots have a negative curvature and thus the apparent values of H_n decrease with temperature. The activation enthalphy for flow can vary by almost an order of magnitude between the melting point and the glass transition, as shown in Table 2 [1].

A formula often used to fit viscosity vs temperature data for inorganic glasses is the Vogel–Fulcher–Tamman (VFT) equation,

$$\log \eta = A + \frac{B}{T - T_0} , \tag{1}$$

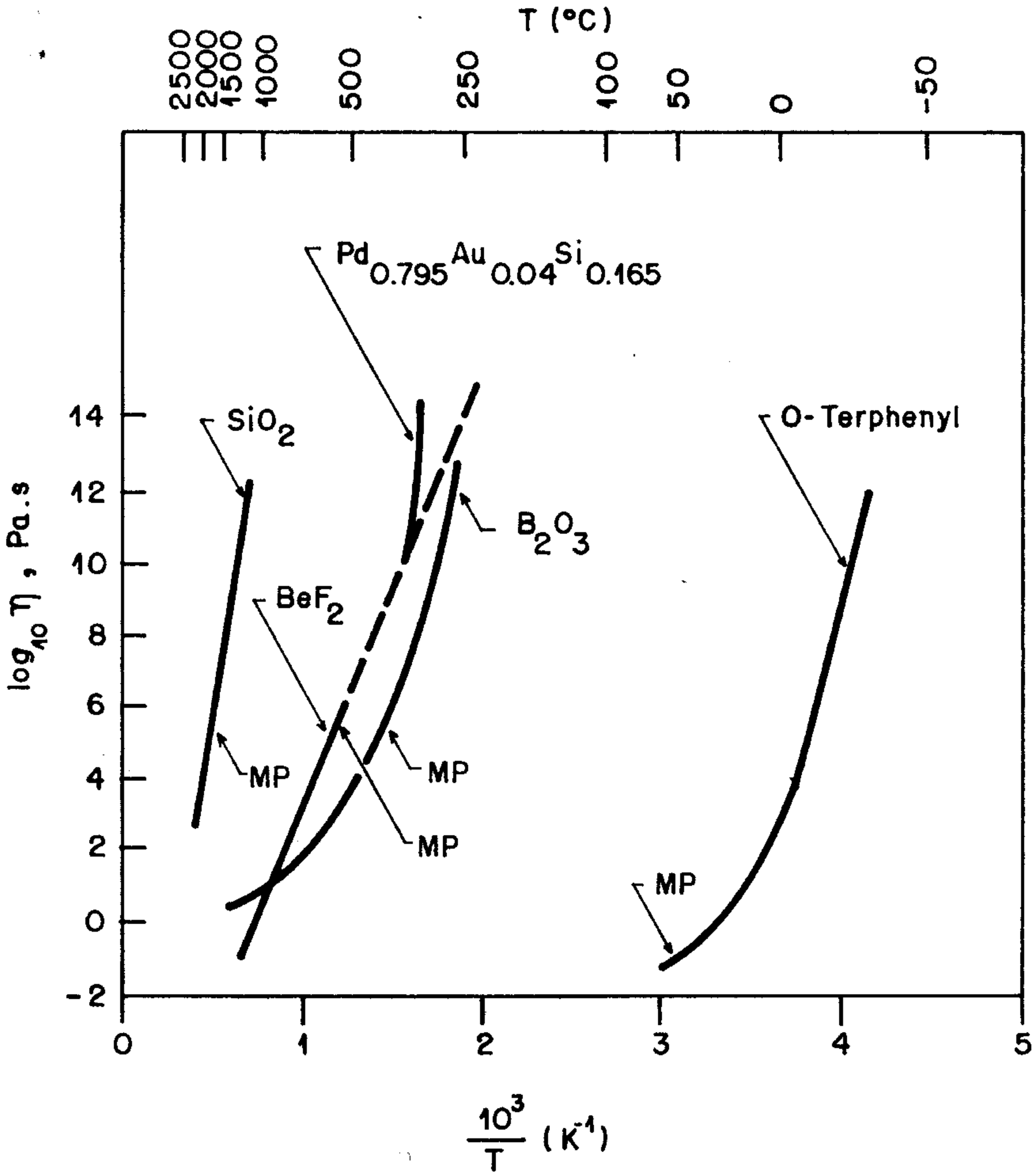

Fig. 1. Viscosities of some good glass-forming liquids (MP = melting point).

where A, B and T_0 are empirical parameters and T is the temperature. Typical values of these constants for stoichiometric oxide glasses were collected by Zanotto [2] and are listed in Table 3.

Thus, at a reduced temperature (T_0/T_m) of approximately 0.45 the viscosity of non-Arrhenian oxide liquids tend to infinity. Caillot *et al.* [3] have also shown that the viscosity of a variety of liquids diverge at a reduced temperature of 0.5. This behavior is predicted by both free-volume and entropy theories of glass transition [1].

Polymer scientists make extensive use of the Williams–Landau–Ferry (WLF) equation,

Table 3. Viscosity parameters for oxide glasses (η, Pa s)

Glass	A	B	T_0 [K]	T_0/T_m
$Na_2O{\cdot}2CaO{\cdot}3SiO_2$	−4.86	4893	547	0.35
$Li_2O{\cdot}2SiO_2$	+1.81	1347	595	0.46
$BaO{\cdot}2SiO_2$	+1.83	1702	795	0.47
$CaO{\cdot}Al_2O_3{\cdot}2SiO_2$	−5.85	6750	738	0.40
$Na_2O{\cdot}2SiO_2$	−0.64	2315	541	0.47
$Li_2O{\cdot}P_2O_5$	−4.10	2000	462	0.50
B_2O_3	−5.02	3665	333	0.46

$$\log \eta = \frac{C_1 T}{C_2 + T - T_g}\,, \tag{2}$$

where $C_1 = 17.2\,\mathrm{kJ/mol}$ and $C_2 = 56.1\,\mathrm{K}$ are universal constants, supposedly valid between T_g and $T_g + 50°\mathrm{C}$ for all polymers.

Several authors hypothesize that the temperature dependence of the activation enthalpy for viscous flow is due to the cooperative motion that must accompany structural changes. This means that the activation enthalpy is not representative of the hopping of single atoms. As the temperature is lowered and the atomic motions become more cooperative, an increasing number of atoms will be involved in flow, and the activation enthalpy will increase. Alternatively, it can be envisaged that the molecular flow units change with temperature thus changing the activation enthalpy.

Indications of structural changes with temperature are only available for a few glasses. For B_2O_3 there is experimental evidence for breaking up of the boroxyl rings with increasing temperature (Walrafen *et al.* [1]). High temperature, X ray data and molecular dynamics simulations also indicate that melt fragility can be correlated to increasing Si–O and Al–O lengths and decreasing Si–O–Si and Al–O–Al angles with temperature, while these parameters are equal for silica glass and liquid, which display Arrhenian behavior.

Finally, it should be stressed that it is not possible to correlate the viscosity activation enthalphy with bond strength. For instance, the energy of vaporization of o-terphenyl is about 75 kJ/mol, whereas H_n at T_g is 490 kJ/mol and H_n at T_m is 65 kJ/mol. The heat of vaporization of BeF_2 is 170 kJ/mol but the activation enthalpy for flow is 240 kJ/mol. For SiO_2, $H_n = 520$–$710\,\mathrm{kJ/mol}$ while the Si–O bond energy is about 440 kJ/mol. The activation enthalphy for oxygen diffusion is about 300 kJ/mol in this same glass.

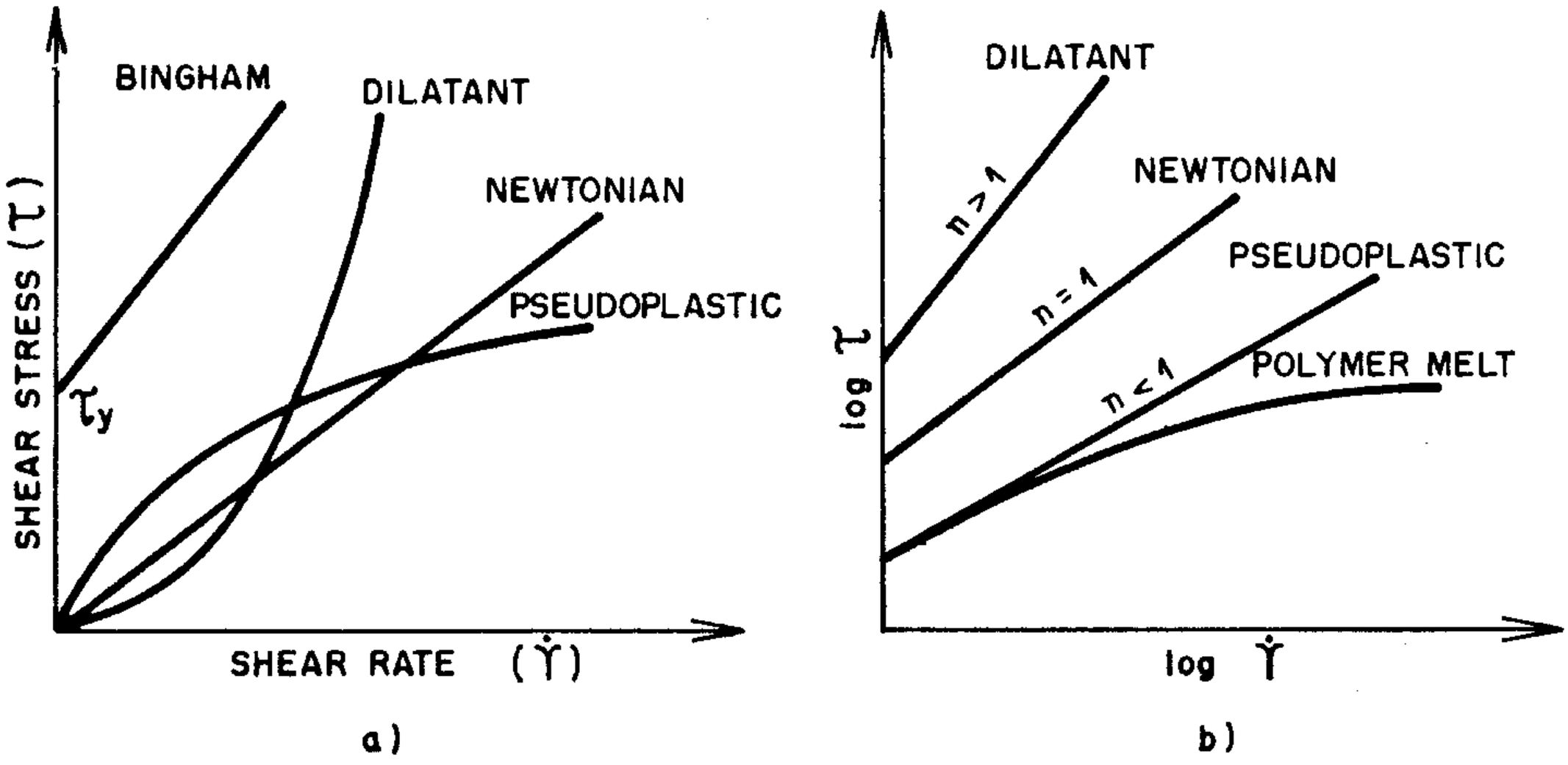

Fig. 2. Rheological behavior of liquids.

7.3 Rheological Models

In a simplified way the rheological behavior of liquids can be represented schematically by Fig. 2.

While polymers are typically pseudoplastic, most oxide glasses are Newtonian, at least for the typical (low) strain rates employed in common forming operations. For a Newtonian liquid confined between two parallel plates, the lower one of which is stationary whilst the upper moves at a constant velocity v_o, the distance between them remaining constant, the liquid velocity is zero at the surface of the lower plate and varies linearly with distance between the plates. A shear stress τ must be supplied to the upper plate to maintain this motion and the coefficient of shear viscosity η, or simply viscosity, is the relation between the applied stress and the velocity gradient dv/dy,

$$\eta = \frac{\tau}{(dv/dy)} \,. \tag{3}$$

In more detail, the flow of glass is more complex due to the combined elastic and viscous response to any type of applied stress, known as viscoelasticity. Several models have been proposed to describe viscoelasticity. Among them, Burger's model has been shown to characterize reasonably well the behavior of inorganic glasses [5]. In this version, illustrated in Fig. 3a, viscous (η_1) and elastic (E_1) elements are combined in series with a Kelvin solid, where two other elements (η_2,E_2) are arranged in parallel and reflect the slow elastic properties. The rate of deformation under constant tensile stress σ and zero initial deformation is made up from the rate of Newton's viscous deformation,

$$\frac{d(\varepsilon_N)}{dt} = \frac{\sigma}{\eta_1} \tag{4}$$

and the rate of deformation of the Kelvin solid

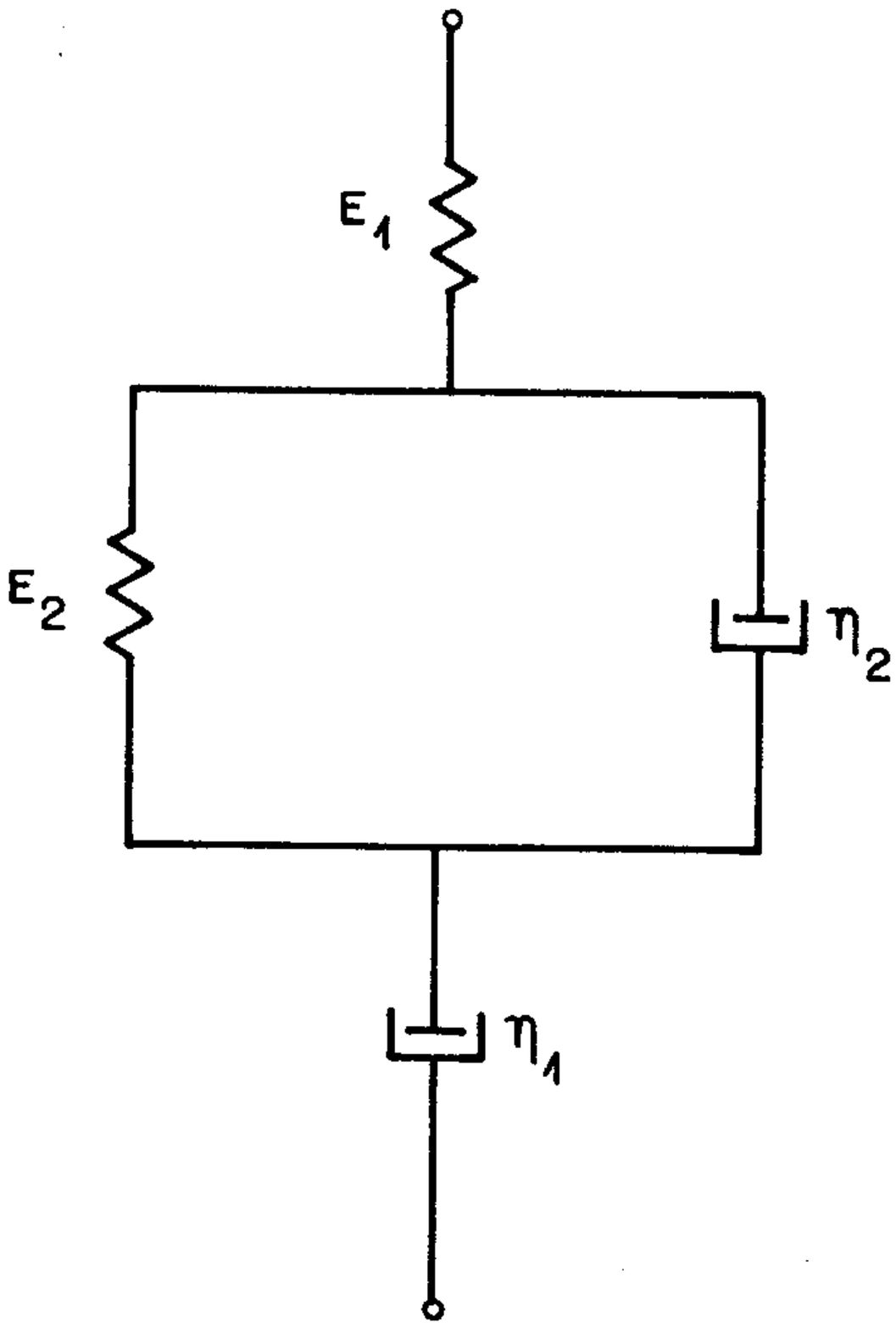

Fig. 3. **a)** Burger's model, **b)** three-parameter model.

$$\frac{d(\varepsilon_k)}{dt} = -\frac{\eta_2}{E_2}\frac{d^2\varepsilon_k}{dt^2} \,. \tag{5}$$

Since

$$\varepsilon_K = \frac{\sigma}{E_2}\{[1 - \exp(-tE_2/\eta_2)]\} \tag{6}$$

for any time

$$\frac{d\varepsilon}{dt} = \frac{\sigma}{\eta_1}\left[1 + \frac{\eta_1}{\eta_2}\exp\left(\frac{-tE_2}{\eta_2}\right)\right] \,, \tag{7}$$

where $\varepsilon = \varepsilon_N + \varepsilon_K$.

The external stress σ and the equilibrium elastic deformation of the whole solid ε_1 are associated by Hooke's law,

$$\sigma = E\varepsilon_1 \,, \tag{8}$$

where E is the elastic modulus of the glass. Thus, when $t \to \infty$ (in practice when $t \gg \eta_2/E_2$) corresponding to Newtonian flow,

$$\frac{d\varepsilon}{dt} = \frac{E\varepsilon_1}{\eta} = \frac{\varepsilon_1}{t^*} \,, \tag{9}$$

An interesting three-parameter model (the Burger model has four parameters) was proposed by Hsueh [6] and is shown in Fig. 3b. He demonstrated that for a Hookean elastic element (E_1) in series with a Kelvin solid (E_2,η), the stress-strain rate relations for constant strain rate and constant stress creep tests are,

$$\sigma(t) = \left(\frac{E_1}{E_2}\right)^2 \eta\epsilon' \left[1 - \exp\left(\frac{-Et}{\eta}\right)\right] + \frac{E_1 E_2 t\epsilon'}{E} \tag{10}$$

where,

$$\epsilon'(t) = \frac{\sigma \exp(-E_2 t/\eta)}{\eta} \tag{11}$$

and,

$$E = E_1 + E_2 \,. \tag{12}$$

It should be emphasized that a constant stress can be achieved only when $E_2 \to 0$ and $t \to \infty$. Note also that the three-parameter model dictates a decreasing strain rate during the constant-stress creep test. To avoid the long loading time required for the conventional creep test and the elaborate instrumentation for the constant stress test, Hsueh [6] suggested an experimental procedure to determine the parameters E_1, E_2 and the viscosity η. Hsueh's technique is appropriate for measuring high viscosities, where elastic effects are more important. In the following section we describe some simpler, more usual methods for viscosity determinations.

7.4 Measurement Techniques

The determination of viscosity is based on the analogy proposed by Trouton [7] between elastic and viscous deformations, where the shear modulus G is substituted by the viscosity coefficient η and the elongation u is replaced by the elongation rate $u' = du/dt$.

The analogy can be appreciated if we refer to the distortion of a rectangular block subjected to a shearing stress (Fig. 4). The relationship between the applied stress τ and the angle of shear γ is $\tau = G\gamma$. If γ is small, $\gamma = du/dy$ and,

$$\tau = G\frac{du}{dy} \tag{13}$$

where u is the displacement of a point in the direction of the applied stress. This has the same form as (3), which defines the viscosity. It should be emphasized here that

$$G = \frac{E}{2(1+\upsilon)} \,. \tag{14}$$

For incompressible liquids, $\upsilon = 0.5$ and thus $G = E/3$.

The range of viscosity of interest in the manufacture and use of glasses and polymers is very wide, varying from 10^0 to 10^{13} Pa s, and thus one has to use more

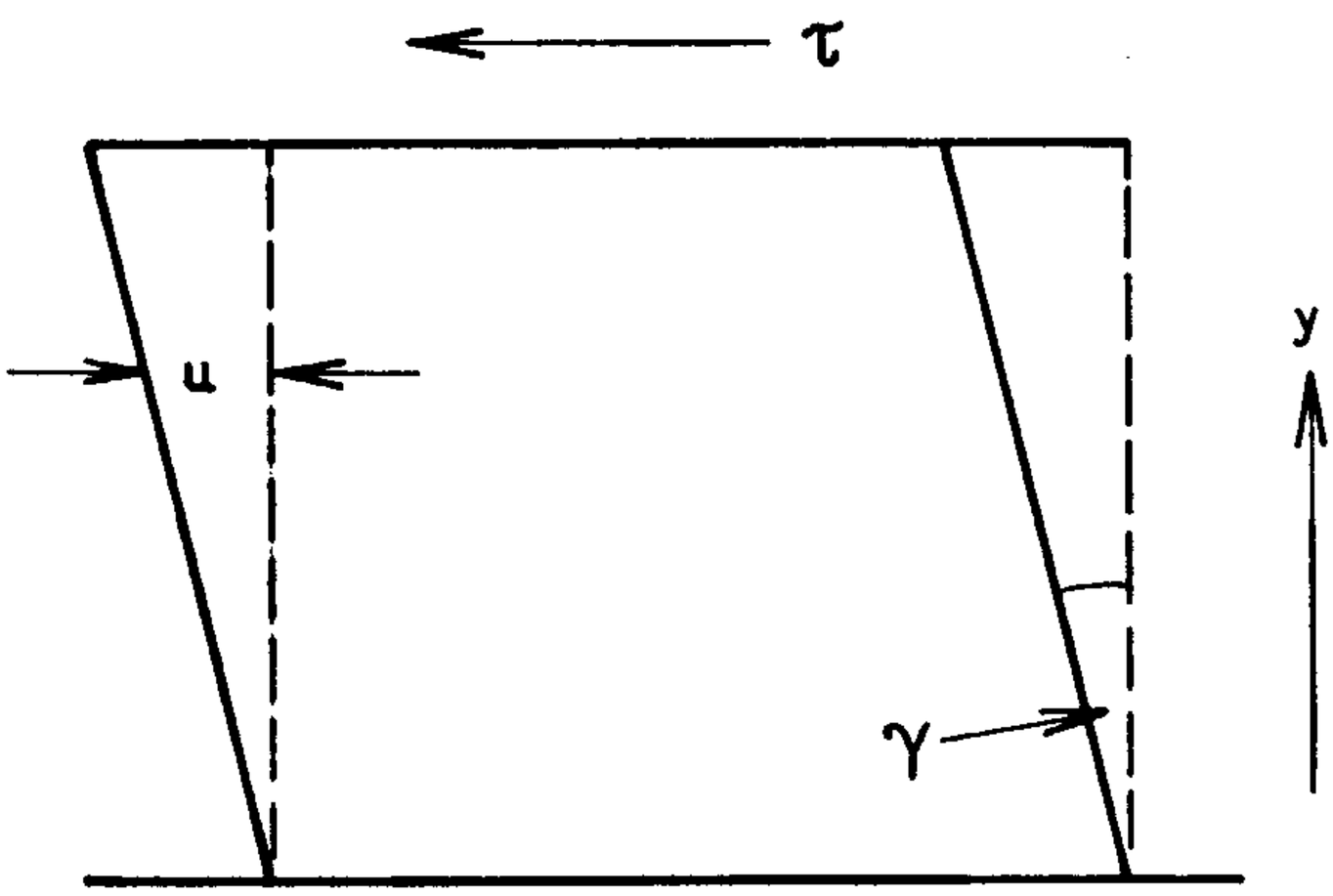

Fig. 4. Solid block under shear stress.

than one method to make measurements over the whole of this range. Hence it is convenient to describe the methods by dividing them into two groups, one group is used for relatively low viscosities ($\log \eta < 5$) and the other for $14 < \log \eta < 5$. Table 4 summarizes the typical viscosity range screened by each method. The actual range measured depends on the instrumental details and can vary by one or two orders of magnitude.

Many other techniques exist to determine the melt viscosity ($\log \eta < 5$) and are extensively used by polymer scientists: sliding plate, poiseuille, rotational plates, dynamic shear, couette, cone-plate, uniaxial flow, etc. These were thoroughly reviewed in several rheology textbooks, see for instance [8] and will not be detailed here. In this chapter we will describe only the main techniques used to determine viscosities in the upper range ($14 < \log \eta < 5$) which have received much less coverage in the literature.

We will demonstrate in the following section that the viscosity can be determined by taking well known equations for the deformation of elastic solids under load and replacing in these equations G or $E/3$ by η to obtain corresponding relations for the rate of elongation of a viscous liquid under load.

Method	Log η [Pa s]
Beam-bending	7–13
Fiber extension	8–12
Cylinder compression	8–12
Penetration	6–12
Parallel plates	4–8
Rotating cylinder	1–7
Counter sphere	1–3

Table 4. Typical viscosity range measured by each method [Pa s].

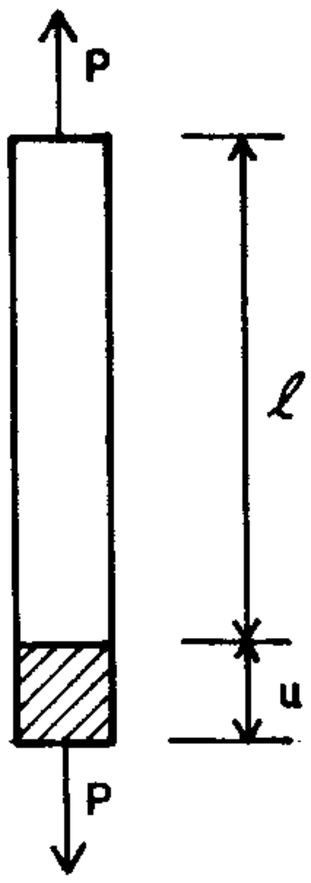

a)

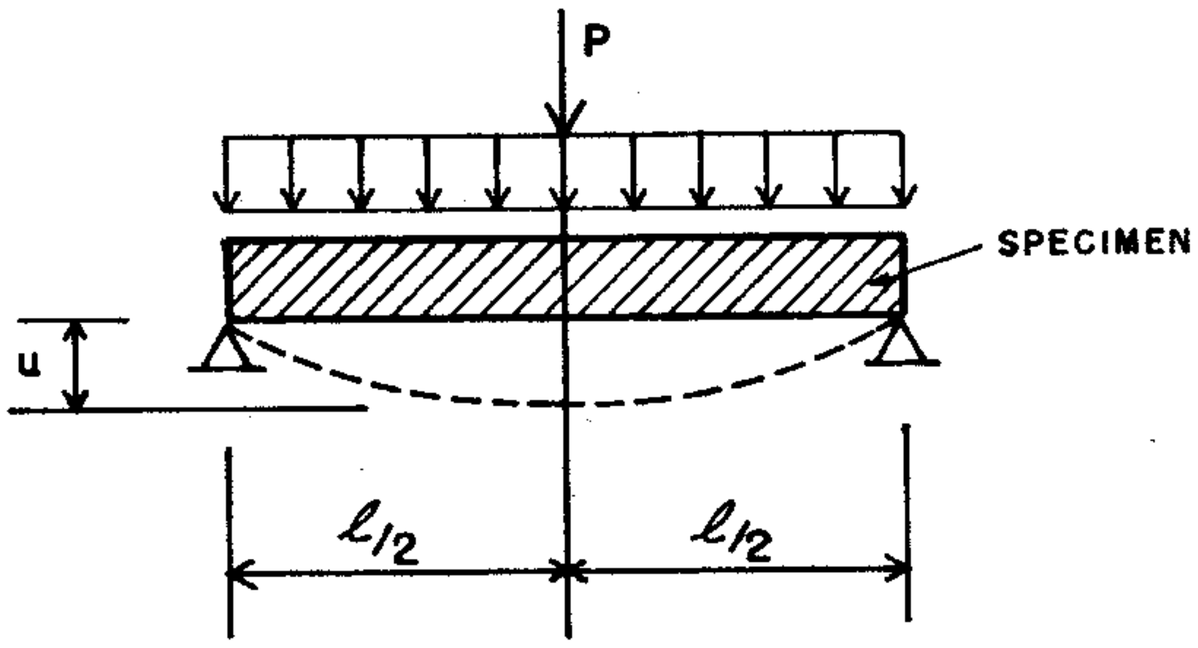

b)

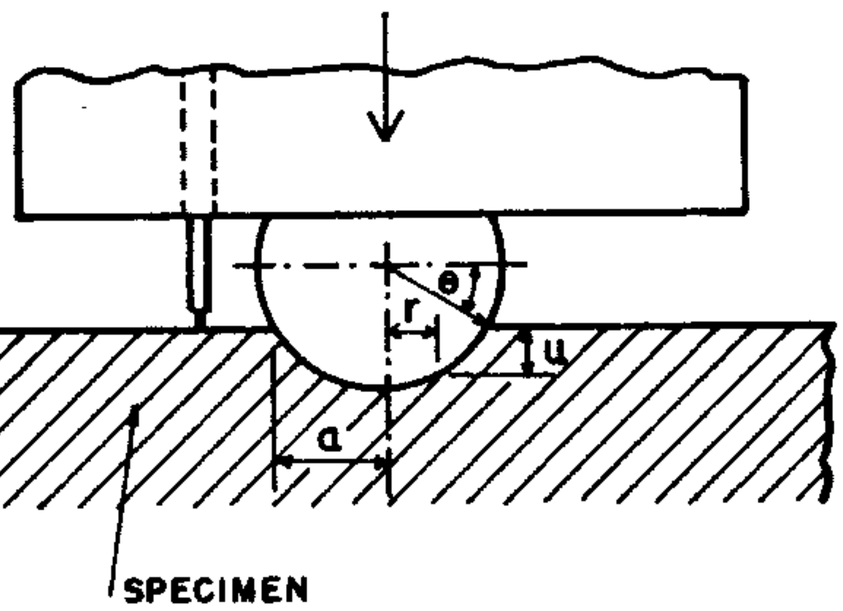

c)

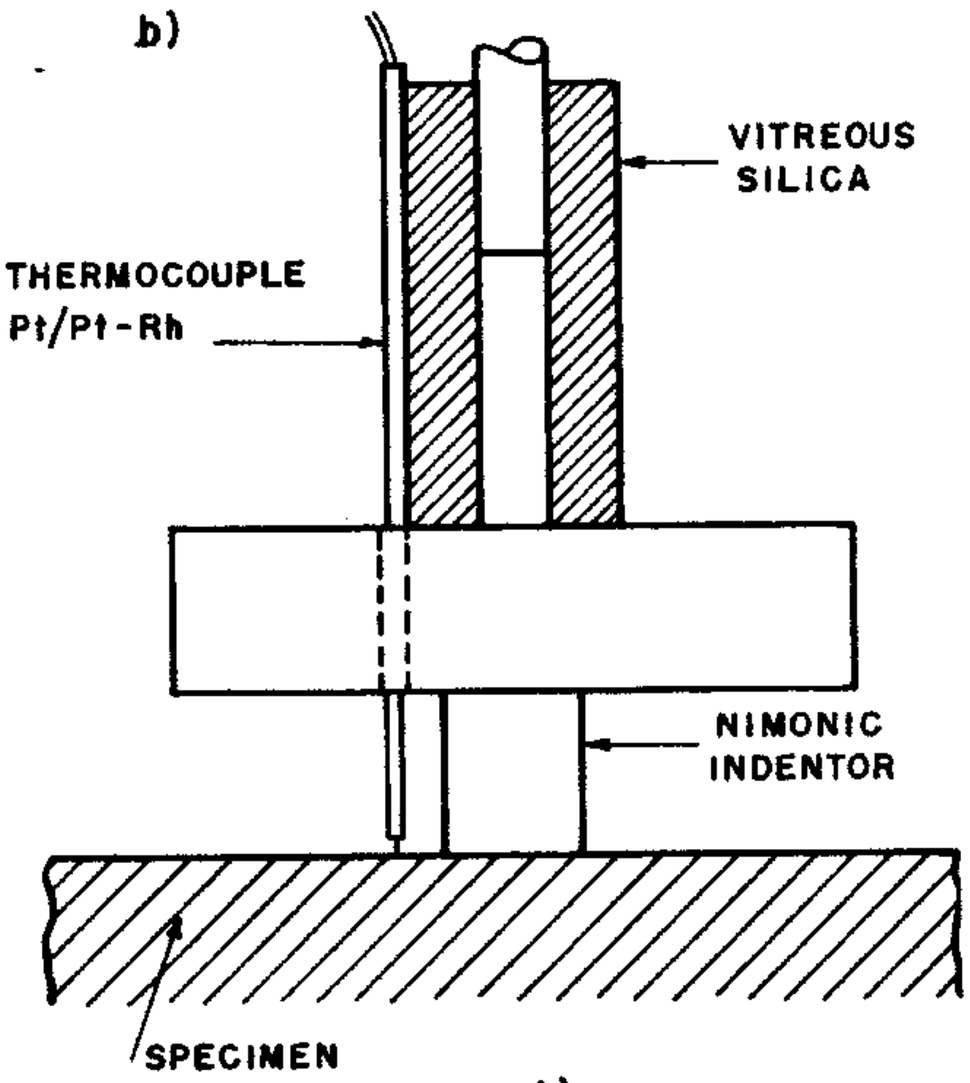

d)

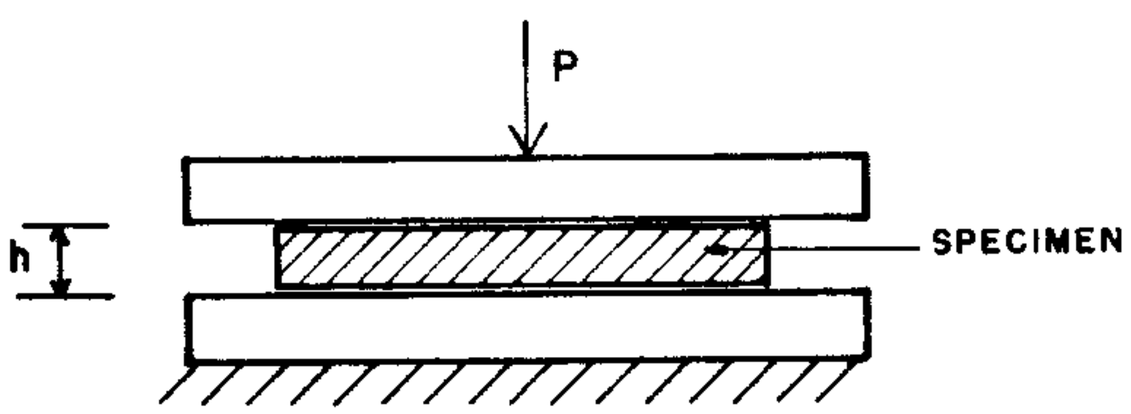

e)

Fig. 5. Schematic diagram for: **a**) fiber elongation, **b**) beam-bending, **c**) spherical indentation, **d**) cylindrical indentation and **e**) parallel plates.

7.4.1 Fiber Extension and Cylinder Compression

The technique of fiber extension was first proposed by Lillie and is now an ASTM standard [9, 10]. Let us assume the geometry depicted in Fig. 5a, i.e a fiber of cross-sectional area A and initial length L, subjected to a uniform force P. If we assume that A does not change significantly for a small elongation and that the mass of the specimen is negligible compared to the external load, the elastic elongation u, is given by,

$$u = \frac{PL}{EA} \,. \tag{15}$$

Thus, by using Trouton's analogy for viscous flow, one has

$$\frac{du}{dt} = \frac{PL}{2\,(1+\upsilon)\,A\eta} \,. \tag{16}$$

If we assume that $\upsilon = 0.5$ and $u' = du/dt$,

$$\eta = \frac{PL}{3Au'} \tag{17}$$

Therefore, to determine the viscosity at a given temperature it is only necessary to know the applied force P, the fiber radius (and thus A) and to measure the elongation rate u'. Thus, one only needs a good furnace with a stable and uniform temperature profile along the fiber length equipped with a LVDT or some other device for measuring deformations. However, it is not trivial to obtain uniform fibers in the laboratory scale. Actually, it is very difficult to obtain fibers of certain materials.

Exactly the same solution is found for the case of compression of cylinders. Hence, one can use commercial dilatometers or thermo-mechanical analyzers to measure the viscosity of cylindrical specimens.

7.4.2 The Beam-Bending Method

The beam-bending method was describes by Jones [11] and Hagy [12] and is now an ASTM standard [13]. A schematic drawing of the experimental arrangement is shown in Fig. 5b, where a specimen of length L and inertia I is symmetrically bent under a weight P. From elasticity theory, the elastic elongation is,

$$u = \frac{PL^3}{48EI} + \frac{5qL^4}{384EI} \tag{18}$$

where $P = mg$ and $q = pAg$ and $I = bh^3/12$. Here, m is the mass, g the gravity, p the specimen density and b and h its lateral dimensions. With the appropriate substitutions into (18) we arrive at,

$$u = \frac{gL^3\,(m + 5pAL/8)}{48EI} \tag{19}$$

By analogy, for viscous flow one has,

$$\eta = \frac{gL^3\,(m + 5pAL/8)}{96\,(1+\upsilon)\,Iu'} \tag{20}$$

Hence, if one knows the specimen geometry and density, the applied load and the deflection rate u', the determination of viscosity is straightforward.

7.4.3 Indentation Techniques

Spherical Indenters. If two elastic spheres of radius R are pressed against each other, it can be shown [14] that the stretching u at a distance r from the center of the contact area (Fig. 5c) is given by

$$u\,(r) = \frac{\left[\pi P_0\,(2a^2 - r^2)\right]\left(\frac{1-\upsilon_1^2}{E_1}\right) + \left(\frac{1-\upsilon_1^2}{E_2}\right)}{4a}\,, \tag{21}$$

where $P_0 = 3P/2\pi a^2$ is the maximum pressure, a the radius of the contact circle and P the applied force. If one of the spheres is much more rigid than the other (this is the case for a metallic indentor on a hot glass, as depicted in Fig. 5c), $E_1 \gg E_2$ and the term $\left(\frac{1-\upsilon_1^2}{E_1}\right)$ vanishes. With the well known relation $E = 2G(l+\upsilon)$, for $r \to 0$, (21) becomes

$$u\,(0) = \frac{3P\,(l-\upsilon)}{8aG}\,. \tag{22}$$

Thus, using Trouton's analogy [7], one obtains

$$\eta = \frac{3P\,(l-\upsilon)}{8au'}\,; \tag{23}$$

where u' is the penetration rate. The radius of indentation a is related to the penetration depth, $u(r=0)$, by $a^2 = u(2R-u)$. Since $a = R\cos\theta$ and $u = R(1-\sin\theta)$, integration of (23) gives

$$\eta = \frac{9P\,(l-\upsilon)\,t}{16\,(2R)^{1/2}\,F\,(u)}\,, \tag{24}$$

where

$$F\,(u) = (2R)^{3/2}\,(\pi - 2\theta - \sin\theta) \tag{25}$$

and

$$\theta = \arcsin\,[1 - (u/R)] \text{ in rad}\,. \tag{26}$$

For small penetrations, $u \ll 2R$ and $F(u) \to u^{3/2}$. However, for small penetration (short times) elastic deformations may still be important and thus flow is not Newtonian and should be described by the more complex equations of Sect. 7.3. Therefore, it is more correct (although more time-consuming) to measure the penetration as a function of time and to compute the value of $F(u)$ to obtain the viscosity rather than using $u^{3/2}$.

Cylindrical Indenters. The elastic stretching u produced by a rigid planar indenter in a semi-infinite plate was deduced by Streicher [15]:

$$u = \frac{c\left(1-\upsilon^2\right)P}{\pi^{1/2}ER} \,, \tag{27}$$

where R is the radius of the cylindrical indenter and $c = 0.96$. Using the Trouton analogy, one has

$$\eta = \frac{c(1-\upsilon)P}{2\pi^{1/2}Ru'} \,. \tag{28}$$

A schematic drawing of indentation by a cylinder is shown in Fig. 5d. This method is interesting because it is capable of covering the widest viscosity range ($13 < \log\eta < 6$) among all the techniques, the specimen geometry is very simple (cylinders or cubes, the only requirement is that their dimensions must be ≈ 5 times larger than the indenter diameter) and the same specimen can be used for several measurements. Finally, commercially available thermo-mechanical analyzers can be used. On the other hand, as far as we know, the indentation techniques are not recognized by the ASTM or any other standardization organization.

7.4.4 Parallel Plates

The parallel-plate technique is schematically represented in Fig. 5e. It is an important method because it covers the intermediate viscosity range, $8 < \log\eta < 4$ (Pa s). The equation which relates the viscosity to the deformation is

$$\eta = \frac{2\pi m h^5}{3V\frac{dh}{dt}\left(2\pi h^3 + V\right)} \,, \tag{29}$$

where m is the applied load, h is the specimen thickness and V is the specimen volume.

7.5 Final Comments

In measuring the viscosity of glass forming liquids, especially in the region of high viscosities where the viscosity varies rapidly with temperature, it is important to pay careful attention to the measurement of temperature. The thermocouple should be placed as close to the specimen as possible and ideally should be in thermal contact with it. The viscometer furnace must be carefully designed so that the entire sample is in a zone of constant temperature. An adequate time should be given at each temperature of measurement to ensure that the specimen has reached an equilibrium temperature before the measurement is made. It is also desirable to maintain a stock of standard materials of homogeneous composition (e.g. the NBS, now NISTC, (USA) makes standard soda-lime, and lead silica glasses), the viscosity of which can be measured from time to time

to ensure that no change has taken place in the apparatus used. This is good practice when making measurements of any physical property.

It is also essential to take into account delayed elastic effects, specially in the neighborhood of T_g. In this case, one has to wait for the relaxation of elastic response before the glass enters into Newtonian behavior. For polymers, which are not Newtonian, one has to determine the viscosity as a function of shear rate. In some instances, the zero shear viscosity is reported, where one extrapolates the viscosity value to zero shear rate.

References

1. S. Brawer: *Relaxation in Viscous Liquids and Glasses* (The American Ceramic Society, Columbus, USA, 1985).
2. E. D. Zanotto: J. Non-Cryst. Solids **89**, 361 (1987).
3. E. Caillot, C. R. Douclot, J. L. Souguet: Acad. Sci. Paris **312**, 447 (1991).
4. C. A. Scamerhorn, C. A. Angell: Geochim. Cosmochim. Acta **55**, 721 (1991).
5. S. V. Nemilov: J. Glass Phys. Chem. [Fizika i Khimiya Stekla] **3**, 148 (1977).
6. C. H. Hsueh: J. Am. Ceram. Soc. **69**, c48 (1986).
7. F. T. Trouton: Proc. R. Soc. Lond. A **519**, 426 (1906).
8. R. Corrieri: in *Melt Rheology* (International School of Advanced Studies in Polymer Science, Ferrara, Italy, 1992).
9. H. R. Lillie: J. Am. Ceram. Soc. **14**, 502 (1931).
10. ASTM Std. C336–71 (1977).
11. J. O. Jones: J. Soc. Glass Tech. **28**, 432–62T (1946).
12. H. E. Hagy: J. Am. Ceram. Soc. **46**, 93 (1963).
13. ASTM Std. C598–72 (1976).
14. S. Timoshenko, J. N. Goodier: *Theory of Elasticity* (McGraw Hill, London, 1951).
15. F. Streicher: Bauin Genier **48**, 949 (1965).